Research on Engineering Structures & Materials
www.jresm.org
Research Group

Research Article

A study on the quantitative recrystallization of cold deformed copper affected by tin-lead solder

Mohammad Salim Kaiser*[1,a], S Reaz Ahmed[2,b]

[1]*Innovation Centre, International University of Business Agriculture and Technology, Dhaka-1230, Bangladesh*
[2]*Dept of Mechanical Eng., Bangladesh University of Engineering and Technology, Dhaka-1000, Bangladesh*

Article Info

Article history:

Received 28 Dec 2023
Accepted 22 June 2024

Keywords:

Cu-alloy;
Sn-Pb solder;
Work hardening;
Recrystallization;
Precipitate;
Microstructure

Abstract

It has been observed that the fractional recrystallization characteristics of commercially pure copper is affected by the presence of individual or both the constituent elements of the Sn-Pb solder alloy. In order to design the experiment, commercially pure Cu, binary copper alloys (Cu-Sn and Cu-Pb) and ternary copper alloy, Cu-Sn-Pb are investigated. Cast alloys are homogenized, solution treated, and then quenched to complete the thermal treatment. In order to recrystallize, alloys are cold rolled to a 75% thickness and then annealed at 700°K isothermally for varying durations, up to 3600 seconds. In this experiment, the fractional recrystallization of annealed samples is evaluated as the normalized difference in microhardness recorded at various time steps. Additionally, in an attempt to verify the experimental results, the well-known Johnson-Mehl-Avrami-Kolmogorov equation is also used to predict the associated recrystallization behavior. From the study, it can be inferred that the presence of Sn-Pb solder-alloy elements have a positive impact on the recrystallization behavior of pure copper due to the solid solution strengthening, in which the effect of tin is greater than that of lead. Quantitative analysis indicates that recrystallization of pure Cu, Cu-Sn, Cu-Pb, and Cu-Sn-Pb alloys attains 99.4%, 95.4%, 98.4%, and 89.5%, respectively. Sn forms intermetallic with Cu but Pb does not. Additionally, Sn forms different intermetallic with impurities and has a BCC crystal structure dissimilar to the FCC of Cu and Pb. As a result, the formation of GP zones and the intermetallic phases during annealing show greater differences in the recrystallization behavior between the two approaches. By combination, microstructural studies of the cold-rolled alloys reveal the elongated grains of the second phases, and the alloys almost completely re-crystallized after 1800 seconds of annealing at 700°K.

1. Introduction

The numerous benefits of copper, including its exceptional electrical and thermal conductivity, resistance to atmospheric corrosion, and antibacterial properties with robust resistance to chemical attack, became more and more significant as industrialization expanded [1-4]. Copper can be combined with an extensive variety of metals to form alloys, and a multitude of alloy systems are currently on the market that allow for the controlled modification of mechanical and technological properties like hardness, tensile properties, and resistance to wear and corrosion [5, 6]. It should be noted that the addition of elements to an alloy can improve certain properties while affecting others in different ways. In the literature, there are lot of information on the influence of alloying elements in copper [2, 4, 6]. For example, alloying with Sn provides strength and precipitation hardening, but reduces ductility and conductivity [7]. The addition of Al shows similar behavior but

*Corresponding author: dkaiser.res@iubat.edu
[a] orcid.org/0000-0002-3796-2209; [b] orcid.org/0000-0002-8382-0711
DOI: http://dx.doi.org/10.17515/resm2024.136ma1228rs

decreases the corrosion properties [8]. When Si is added, it improves tensile strength as well as machineability but is less corrosion-resistant than other types of Cu alloys. While Ni-added alloys have high thermal stability, which enables them to keep their mechanical characteristics even at high temperatures, but their machinability is a result of their high toughness [3, 9]. Alloyed with Zr refines the grain structure and thermal stability of the alloys, and Sc furthermore provides precipitation strengthening [10, 11]. High conductivity, including thermal and electrical conductivities, and high strength are the two most desirable characteristics of high-performance copper alloys. Such property profiles could have a wide range of present and future uses in automotive and electronic industries, including busbars in commutators, casting molds, die-casting plungers, electric motors, generators, relays, switches, and welding electrodes. When Cu is used as the primary conductor in the above electrical sector, wires or parts are to be joined by using solders. Note that, at earlier stages, Sn-Pb solder alloys are mostly used for the joining processes. Therefore, the corresponding recycled copper would contain a small amount of Sn-Pb solder elements as well as trace impurities [12, 13].

Once more, it might be suggested that using copper purposefully or under certain conditions requires plastic deformation. It is established that cold working is a simple and common method to improve strength by changing the crystal structure of common materials. When alloying elements are added, the quality of the improved strength of the base material varies. Obviously, the presence of Sn-Pb solder will play an important role in strength through significant dislocation hardening and grain refinement [3, 14, 15]. When worked again at a high temperature beyond half of its melting temperature, a group of processes known as recrystallization can release the stored energy, the deformed grains are replaced by a new set of original defect-free grains, etc. As a result, radically decrease in strength [16-18]. Once it comes to pure metals, the single crystal's original orientation determines the values of stored energy and recrystallization temperature. When elements are present in small amounts, they can occasionally have the opposite effect of pure metals, increasing the recrystallization temperature and reducing the stored energy. This depends on the properties, quantity, and rate of deformation of the elements [19, 20].

There is no mention of the copper's reusable qualities, especially when affected by Sn-Pb solder. In order to thoroughly study and appropriately identify the engineering applications of scraped Cu for optimal exploitation toward the advancement of civilization, it is necessary to discover a number of its qualities. Recrystallization behavior is one of them. It may be investigated in several ways. Dynamic and isothermal resistivity measurements have been used by previous researchers to examine this attribute [21]. The most straightforward way to investigate the behavior of recrystallization is to use optical microscopy to calculate the fraction that has been recrystallized [22]. Vickers microhardness techniques and differential scanning calorimetry may also be used to investigate it [23]. It is challenging to discern between the recrystallized and deformed microstructures in severely deformed copper, though, the recrystallized fraction has also been ascertained by other indirect techniques. Considering all circumstances, microhardness data is the easiest procedure to determine the fractional recrystallization of the materials [24]. Consequently, the focus of this study is on how Sn-Pb solder affects the fractional recrystallization behavior of copper that has undergone significant plastic deformation. To compare and isolate the effect of individual elements on the recrystallization behavior, the same reduction ratio and subsequent annealing are employed for commercially pure Cu, Cu-Sn, and Cu-Pb alloys. It also takes into account the specific amounts of Sn and Pb based on the composition of the solder. Another, since the Johnson-Mehl-Avrami-Kolmogorov (JMAK) relationship follows the isothermal kinetics of the recrystallization process of the specific material system, an effort is made to analyze

and compare the results of the experimental study derived from the difference in micro-hardness values for these trial alloys [25].

2. Experimental Methods

2.1. Preparation of Alloys

To prepare the copper-solder alloy (Cu-Sn-Pb), copper wires as well as soldered connecting structures after extensive use were collected from various sources, which was then melted using a suitable flux cover in a pit furnace powered by natural gas in a traditional manner. Optical emission spectroscopy has shown that the resulting cast copper contains trace amounts of lead and tin as well as few other elements with negligible amount. It was a Cu-Sn-Pb alloy composed of about one percent each of tin and lead. Simultaneously, based on the above minor alloying elements, three more samples of commercially pure Cu, Cu-Sn, and Cu-Pb were prepared to establish the impact of individual components of the solder. The chemical compositions of the major element are listed in Table 1, in which the negligible elements, like, Si, Fe, P, etc., are not included. One can however see from the table that the binary alloys, that is, Cu-Sn and Cu-Pb contain negligible amounts of Pb and Sn, respectively.

Table 1. Alloy chemical composition by wt.%

Alloy	Cu	Sn	Pb
Pure Cu	99.986	0.0	0.0
Cu-Sn	98.456	1.134	0.012
Cu-Pb	98.433	0.002	1.197
Cu-Sn-Pb	97.113	1.257	1.195

2.2. Preparation of The Test Specimen

The above four cast samples were homogenized for eight hours at 773°K and air-cooled to allow the release of internal stresses and to achieve the equilibrium conditions of solidification. Again, the solution treatment was done at 973°K for two hours and quenched into ice-salt water to get a super saturated single-phase region. To apply cold rolling, the samples were machined to assume the dimension of 300 × 15 × 12 mm. The cold working operation was then performed using a laboratory-scale 10HP cold rolling machine under 1 mm reduction per pass. Consequently, the samples' thickness decreased from 12 mm to 3 mm as they deformed by 75%. To study the recrystallization behavior, isothermal annealing of cold rolled samples was performed for a duration of 3600 seconds at 700°K. Additionally, all four samples were annealed at 773°K for four hours to achieve a fully recrystallized state [12]. For different tests, the finished surface was prepared with sandpaper and polished to a size of 15 x 15 x 3 mm.

2.3. Working Instruments and Test data collection methods

2.3.1 Hardness Test

A Mitutoyo HM-200 Series 810-Micro Vickers Hardness Testing Machine was used to measure the hardness of various alloys at various annealed conditions. Diamond Indenter was applied to the sample with a load of 100 grams for a dwell time of 20 seconds. On each polished surface of the aged samples, at least eleven indentations were made at various locations of three test specimens prepared from each of the four categories.

2.3.2 Resistivity Measurement

The electrical conductivity of alloys under various conditions was measured using an Electric Conductivity Meter (type 979). In order to plot the graph, the conductivity data

was then converted to electrical resistivity. Likewise the case of hardness, a minimum of eleven measurements were taken at different places on each polished surface of three test specimens prepared from each of the four categories.

2.3.3 Microstructural Study

Finally, to ascertain the microstructure and granular texture of the materials, an optical microscopic observation was performed on the cold rolled and annealed samples. An OEM BW-S500 optical electronic microscope was used for this study. The samples were ultimately polished with alumina to reveal the microstructure. The same combination of ammonium hydroxide and hydrogen peroxide (3%) was employed for metallographic copper etching. In addition, the surface morphologies of deformed samples were investigated with the help of a field emission scanning electron microscope model JEOL JSM-7600F. An electron dispersive spectrometer (JEOL EX-37001 model) connected to the setup to capture the samples' EDX spectra. Microstructural images were taken at different locations of the sample with various magnifications, and the representative images are presented.

3. Results and Discussion

3.1. Isothermal Annealing

Figure 1 shows the change in average microhardness over time of commercially pure Cu, tin-doped binary Cu alloy (Cu-Sn), lead-doped binary Cu alloy (Cu-Pb), and the ternary Cu alloy, Cu-Sn-Pb under isothermal annealing at 700°K. The harness values corresponding to the initial state, that is, at zero time, represent the harness of 75% cold-rolled samples without any influence of annealing. It is clearly demonstrated that all alloys soften with time at different rates. Copper shows a relatively rapid and steeper decrease in hardness following a more or less constant value at higher time durations. The alloy samples also exhibit variation in hardness and follow trends nearly similar to that of pure Cu, although some variations may be noticed in higher time domain ($1200 \leq t \leq 3600$ sec). From the results it is observed that, at the steady-state condition (higher time domain) pure Cu assumes the lowest and the ternary alloy the highest hardness, and the hardness of the binary alloys remain in between. More specifically, tin is identified to be more influential than lead in assuming higher hardness of the binary alloys in the steady-state condition. All the samples were plastically deformed by 75%.

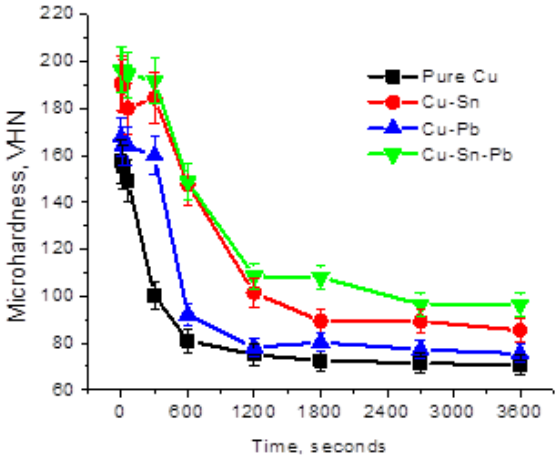

Fig. 1. Microhardness variation, isothermal annealing at 700°K

A highly cold deformed alloy consists of huge dislocations, which result in its developed hardness. Hardness reduction in the early stages of annealing may be associated with rearrangement of dislocations as well as stress-relieving and higher annealing times for recovery, recrystallization, and grain growth [12, 26]. An elevated temperature during annealing for any metal that has been deformed and hardened will eventually nullify the effect of strain hardening. Formation of a defect free new grain structure during the recrystallization process is the primary cause of softening [27, 28]. Initially, higher hardness is observed for minor-added alloys compared to pure copper because the solid solution is strengthened through the Sn and Pb phases. The higher hardness of the Sn-added alloy is due to its BCC crystal lattice, which differs from that of Cu's FCC crystal lattice, and Pb has a similar FCC crystal lattice to Cu. The FCC and BCC lattice alloys exhibit different supersaturated solid solution patterns of higher internal stress than those of both similar lattices. One thing may be noted that atomic size of the Sn is higher than Pb as well as Cu. As a result, the addition of Sn to the Cu matrix accelerates the internal stress. The Pb element does not form any intermetallic with Cu. Nonetheless, Sn not only forms different intermetallic with Cu, but it also forms intermetallic with other negligible impurities as deposited during casting, which play an important role in strengthening the alloy [13, 29, 30]. The main stable intermediate phases are Cu_3Sn, $Cu_{41}Sn_{11}$, $Cu_{10}Sn_3$, and Cu_6Sn_5, where Cu_3Sn and Cu_6Sn_5 two intermetallic, primarily have a significant impact on hardness [31]. Solder affected alloys bear the highest hardness for both alloying effects. At the initial stage of annealing, the element added alloys show a fluctuating nature of hardness due to the formation of different intermetallic. These intermetallic hinder the dislocation movement during the annealing, so such a type of nature is observed.

3.2. Recrystallized Fraction

In general, the maximum and minimum values of hardness represent the important characteristics of any material's microstructure; therefore, recrystallization kinetics may be expressed in terms of fractional softening, as demonstrated by earlier researches [26, 32]. Following the standard procedure of the above literature, the fractional recrystallization, *X* is defined as the ratio of change in hardness, which is as follows:

$$X = \frac{H_{max} - H_i}{H_{max} - H_{min}} \tag{1}$$

Where, $H_{\max}$ and $H_{\min}$ represent the maximum and minimum hardness corresponding to the initial cold-rolled and the completely recrystallized state of the sample, whereas the hardness at any time step after applying thermal annealing is denoted by H_i. For the present material, no change in hardness is encountered at time intervals of 2, 4, 6, 8 hours, for example, after applying annealing at 773°K, which basically represents the state of full recrystallization, which has also been found in the work of reference [12]. Table 2 lists the maximum and minimum microhardness values of the experimental alloys under two conditions: unannealed and annealed for four hours at 773°K. Fig. 2 shows the variation of fractional recrystallization, *X* for the four samples annealed at 700°K as a function of annealing time, which is obtained based on Eq. (1) and Table 2. According to the figure, copper has the largest percentage of recrystallization. Pb-doped and Sn-doped Cu alloys as well as the Cu-Sn-Pb alloy respectively follow the gradually decreasing trends of recrystallization. The above recrystallization behavior of the alloys may be realized by the formation the different intermetallics that hinder the dislocation movement of the alloys. Note that it has already been discussed about the influence of individual and both the elements of Sn-Pb solder on the microhardness under annealing treatment. Similar observations were also found for other trace or minor added alloys [33].

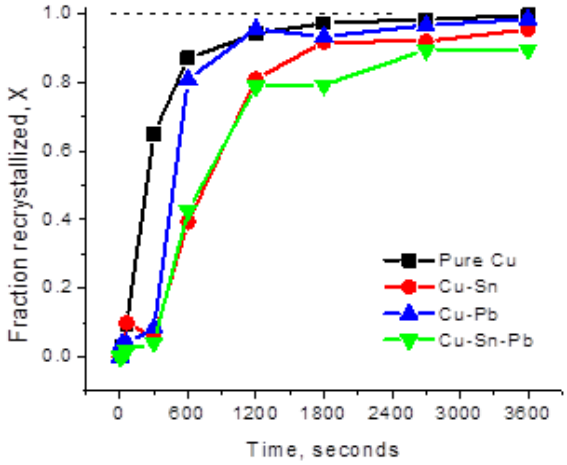

Fig. 2. Difference in the kinetics of recrystallization with annealing time derived from microhardness data

The Johnson-Mehl-Avrami-Kolmogorov model (JMAK equation) may be used to investigate the kinetics of a material's recrystallization [32, 34]. In order to theoretically study the fraction recrystallization as a function of annealing time, the JMAK equation can be stated as:

$$X = 1 - exp[-(kt)^n] \tag{2}$$

where t is the applied time for annealing, and k and n are the temperature dependent constants and the JMAK exponent, respectively. The parameters are contingent upon the conditions of the material and processing. Following a logarithmic operation, the JMAK equation can be reduced to a linear relationship as follows:

$$ln[ln(\frac{1}{1-X})] = nln(t) + nln(k) \tag{3}$$

When plotted on a logarithmic scale, ln{1/(1 − X)} vs. t should show a straight line. The parameters can be obtained from Fig. 3 by way of the linear relationship whose slope is equal to the JMAK exponent. The kinetics of recrystallization of alloys annealed at 700°K can be obtained using the values of the JMAK exponent n and parameter k. The comparison of recrystallization kinetics for commercially pure Cu, binary tin, and lead-added alloys, as well as ternary tin-lead solder affected alloys obtained micro-hardness data and JMAK type investigation, is shown in Fig. 4-7. The experimental alloys exhibit different softening under annealing treatment and, as a result, exhibit varying slopes for their recrystallization performance.

$$X = 1 - exp[-(0.002114 \times t)^{0.98744}] \textit{ for pure Cu} \tag{4}$$

$$X = 1 - exp[-(0.000894 \times t)^{0.99975}] \textit{ for Cu-Sn alloy} \tag{5}$$

$$X = 1 - exp[-(0.001292 \times t)^{1.02257}] \textit{ for Cu-Pb alloy} \tag{6}$$

$$X = 1 - exp[-(0.000705 \times t)^{1.37267}] \textit{ for Cu-Sn-Pb alloy} \tag{7}$$

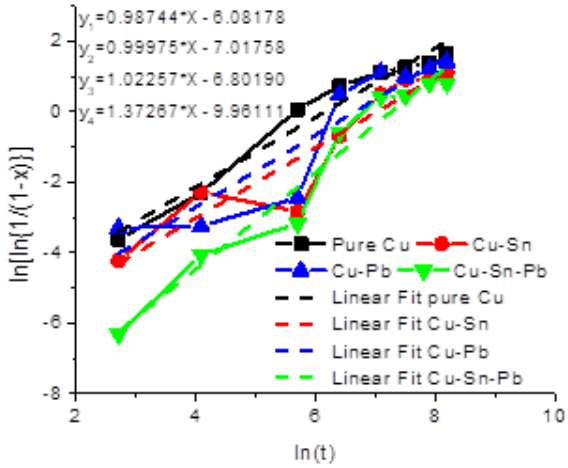

Fig. 3. Plot of ln{1/(1-X)} Vs. (t) in logarithmic scale, to obtain linear relationship

Table 2. Measured maximum and minimum microhardness of alloys with JMAK exponent

Alloy	H_{max}	H_{min}	n	k
Pure Cu	157.3	70.0	0.98744	0.002114
Cu-Sn	190.8	80.3	0.99975	0.000894
Cu-Pb	167.6	74.0	1.02257	0.001292
Cu-Sn-Pb	196.4	84.7	1.37267	0.000705

The experimental Cu sample displays the lowest disparity among two methods of fraction recrystallization (Fig. 4). Doped by Sn and Pb alloys, there are the higher differences between the two respective methods, as seen respectively in Fig. 5 and Fig. 6. The reason for this phenomenon is that the finely dispersed particles typically slow down the process of recrystallization, which has a greater slowing effect on nucleation than on growth.

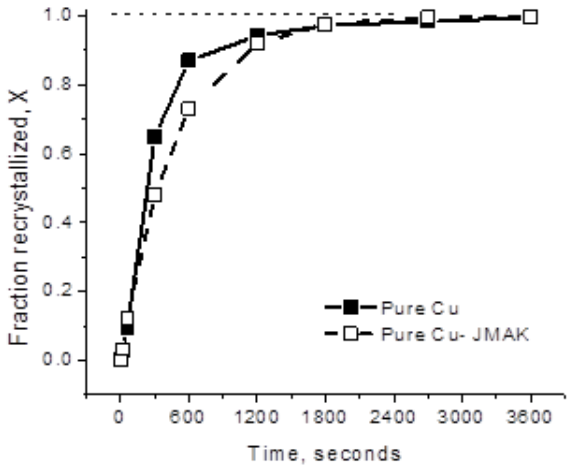

Fig. 4. Inconsistency of recrystallization kinetics determined by both JMAK type study and micro-hardness data for commercially pure Cu

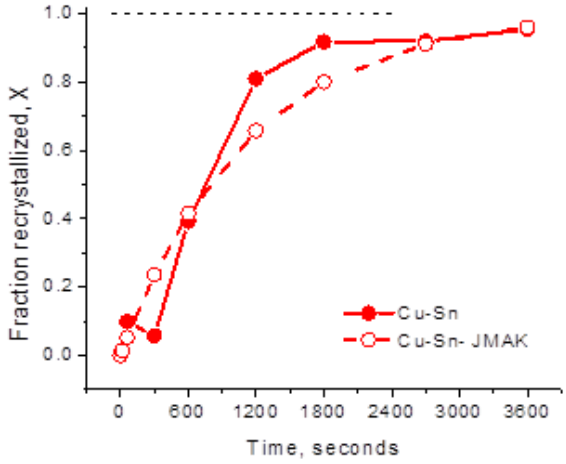

Fig. 5. Inconsistency of recrystallization kinetics determined by both JMAK type study and micro-hardness data for Cu-Sn alloy

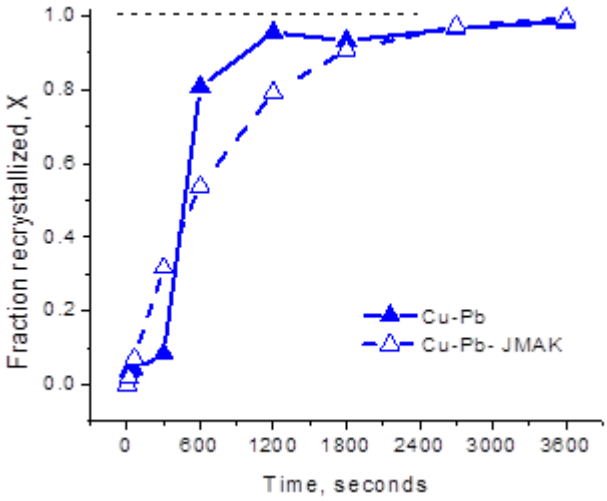

Fig. 6. Inconsistency of recrystallization kinetics determined by both JMAK type study and micro-hardness data for Cu-Pb alloy

Consequently, the orientation dependent nucleation provides a rationale for the texture changes. In the case of commercially pure Cu, trace impurities may be exerted from the melt environment during casting, which forms an insignificant amount of intermetallic during the process of annealing, so some effect may be felt [18, 35]. In the case of Sn addition, dissolution of different phases and different intermetallic formations with Cu and impurities in the course of annealing treatment make the differences higher [31]. Pb addition shows a relatively low value as it does not form any intermetallic with copper. Solder-affected alloy displays the maximum variation because of the presence of both elements (Fig. 7). Finally, it can be summarized that Eq. (1) describes the experimental results of fractional recrystallization based on the actual measurements of hardness, whereas the JMAK equation gives the corresponding theoretical prediction of the behavior.

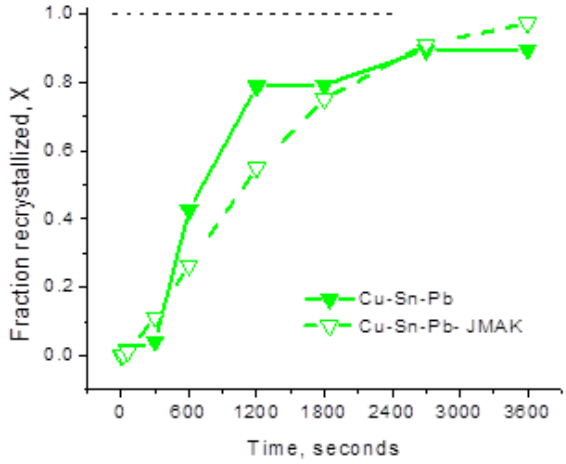

Fig. 7. Inconsistency of recrystallization kinetics determined by both JMAK type study and micro-hardness data for Cu-Sn-Pb alloy

A comparison of the results shown in Figs. 4-7 reveals that, the discrepancy between the two approaches is basically observed in the early stages of the annealing treatment, showing good agreement in the steady-state regions. It can be noted that, for annealing under such higher temperature, the formation of intermetallic occurs within a very short period of time, which would be the probable reason for the above discrepancy.

3.3 Resistivity

In this section, the electrical resistivity of pure copper as well as its binary and ternary alloys is recorded in an attempt to assess the electrical conduction characteristics of the alloy samples during the process of fractional recrystallization as a function of annealing time. The resistivity curves of the alloy samples at the same annealing condition mentioned earlier are presented in Fig. 8, which show an initial drop, followed by a small increase, and finally a slow but steady decrease of resistivity. During isothermal ageing of the test alloys, the first drop in resistivity occurs due to dislocation rearrangement as well as the recovery phenomena of the cold-worked alloy.

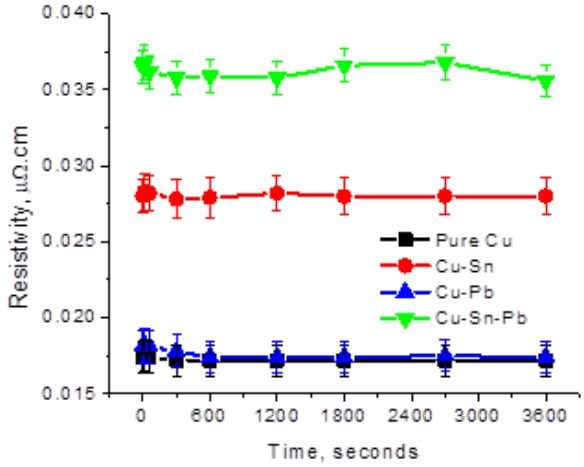

Fig. 8. Resistivity fluctuation, isothermal annealing at 700°K

The rate of resistivity reduction is the highest for solder-affected alloy because they consist of the highest dislocation density created by both elements. The second minor increase in resistivity of all alloys is linked to different intermetallic formations. The fine precipitate inhibits free electron movement, resulting in increased resistivity in alloys. The chemical composition previously stated that during the casting process, all alloys consist of different trace impurities, so they form different intermetallic through heat treatment. In the final stage of annealing, there is a slow and steady decrease in resistivity due to the following factors: particle coarsening, grain coarsening, and recrystallization, ultimately resulting in a decrease in electron anomalous scattering [36, 37]. Again, Sn added alloy normally demonstrates all the cases of higher intensity than Pb-added alloy and pure Cu has the lowest. Since Sn has a BCC lattice difference from the Cu FCC lattice, the lattice distortion is higher than that of the FCC Pb alloy. Additionally, Sn forms different intermetallic with Cu and trace impurities, resulting in a higher alloy resistivity than Pb. The alloy that is affected by the solder has an impact, which demonstrates the resistive effect of both elements.

3.4 Optical images of Grains

Optical micrographs of commercially pure Cu, tin-added Cu-Sn, lead added Cu-Pb, and solder affected Cu-Sn-Pb alloys at the combination of solution treated and cold-rolled by 75% are displayed in Fig. 9a-d. Every single grain in the microstructure is heterogeneous and distributed in rolling directions. Extensive plastic deformation destroys grain boundaries to form sub grains. A minor addition of elements does not provide the foremost differences. But some deviations can be distinguished between alloys, as grain boundaries are relatively thin for Cu, followed by Pb-doped, Sn-doped and solder-affected alloys. Copper materials contain the minimum number of impurities, such as Fe, C, P, etc., so the intermetallic are smaller in both size and quantity during solution treatment. Tin forms denser grain boundaries than lead because alloys with FCC Cu and BCC Sn lattices exhibit different supersaturated solid solution patterns than similar lattices of both Cu and Pb. Additionally, the atomic size of Sn is larger than that of Pb as well as Cu, so it tends to be allocated to grain boundaries, resulting in denser grain boundaries for alloys containing Sn. Both material effects dominate the dense boundary of the solder affected Cu [38]. After 30 minutes of annealing at 700°K, the appearance of the alloys' microstructures entirely changed. The microstructure completely lacks elongated grains; most residual phases dissolve into the α-Cu matrix, the grain boundaries are clearly defined, and the grain outlines are equiaxed (Fig. 10a-d).

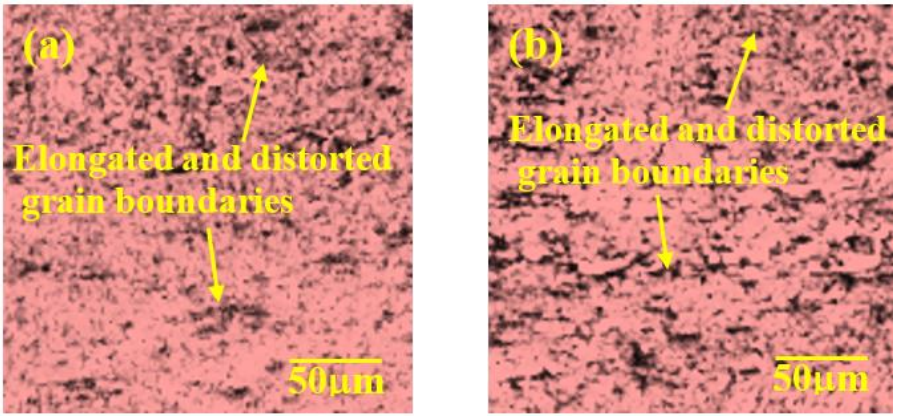

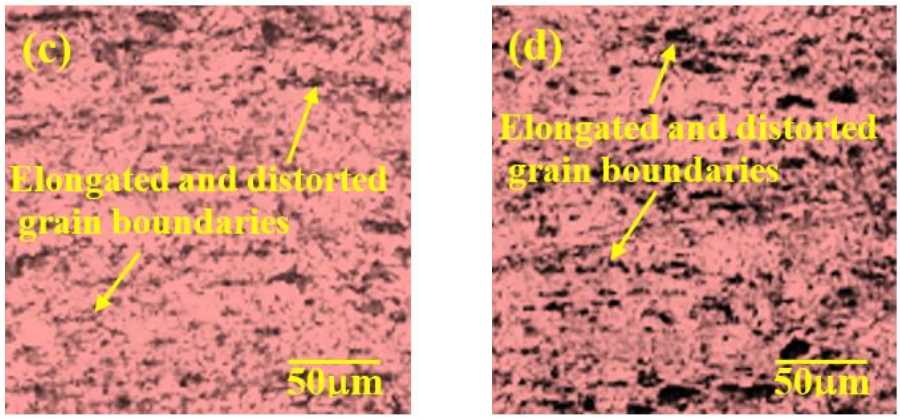

Fig. 9. Optical images of cold rolled (a) pure Cu, (b) binary Cu-Sn alloy, (c) binary Cu-Pb alloy and (d) ternary Cu-Sn-Pb alloy

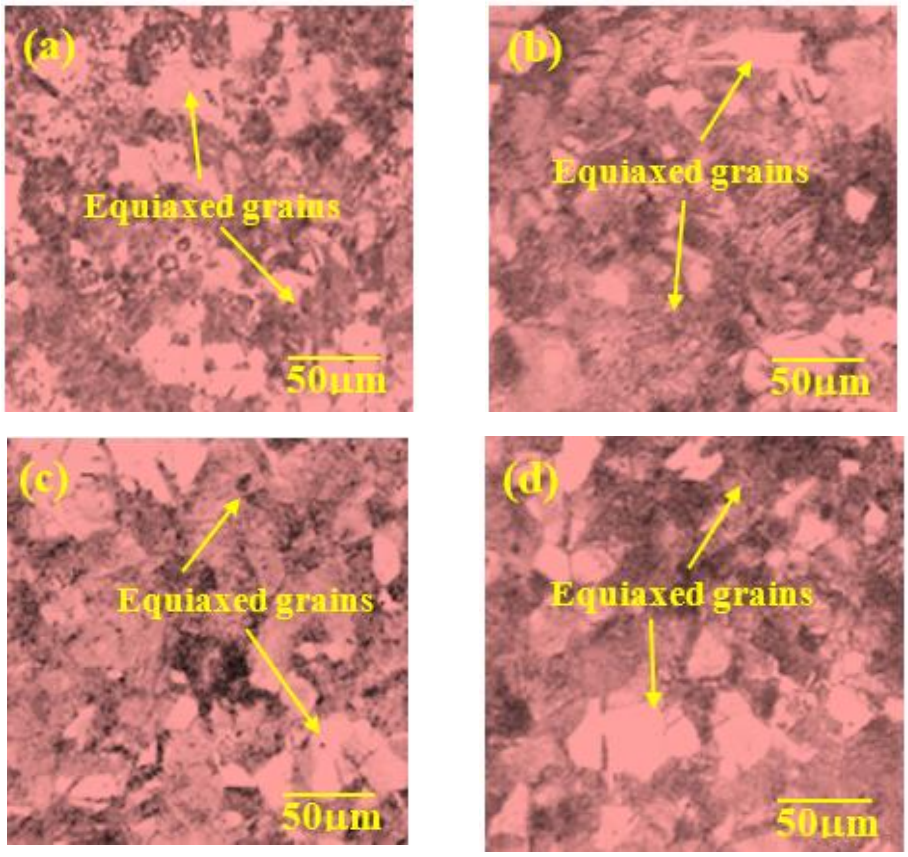

Fig. 10. Optical images of cold rolled (a) pure Cu, (b) binary Cu-Sn alloy, (c) binary Cu-Pb alloy and (d) ternary Cu-Sn-Pb alloy annealed at 700°K for 1800 seconds

The alloys contain a variety of trace impurities and small additional elements that can form intermetallic particles during the casting and annealing processes. However, most of these

precipitates are distributed along grain boundaries at higher annealing temperatures and times. For phases containing elements of Si and Fe, the dissolution temperature is very high. These phases are so tiny that they can still be found inside grains and next to grain boundaries [6].

3.5 SEM and EDX Analysis

In order to comply with the optical microstructure, the SEM images and the respective EDX spectra of cold-rolled alloys are shown in Figure 11a-d. The EDX spectra are included mainly to demonstrate the elemental analysis of the SEM images of pure copper and its alloys. Due to plastic deformation, equiaxed grains elongate regularly in the rolling direction. For severe deformation, the crystal grains become blurred, and the crystal grains are difficult to distinguish. Thus, the microstructure of pure Cu consists of the solid phases of α-Cu and insignificant intermetallic produced by trace impurities. The alloy microstructure of tin is composed of primary copper, β-tin, and various impurity intermetallic. Since it has the BCC crystal structure, which is different from the FCC of Al, it tends to distribute at grain boundaries, resulting in dense grain boundaries. Similarly, alloys containing lead show primary aluminum, α-lead, and impurities distributed in the microstructure. But grain boundaries are not very thick because both Pb and Al alloys have the FCC crystal structure. The solder affected alloy reflects the addition of both elements [31].

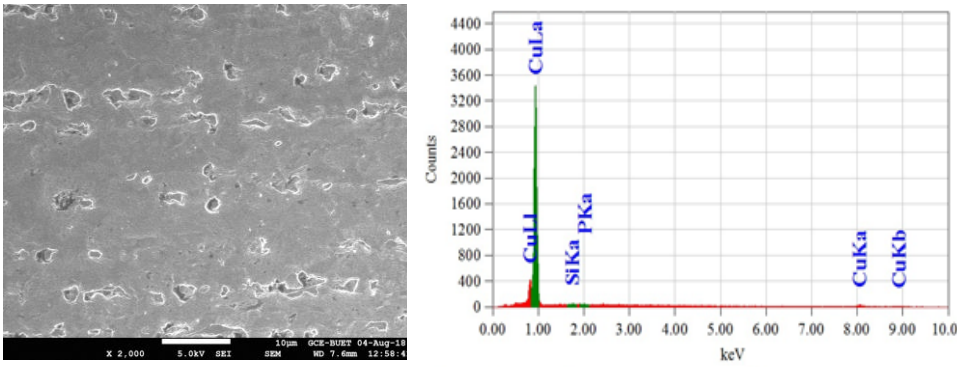

(a)

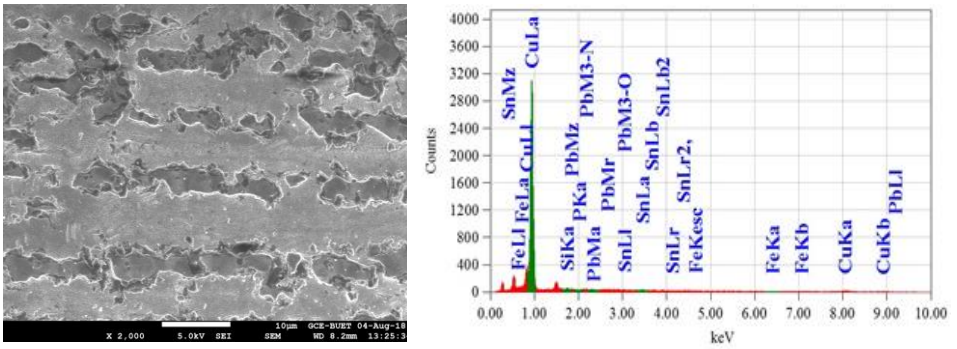

(b)

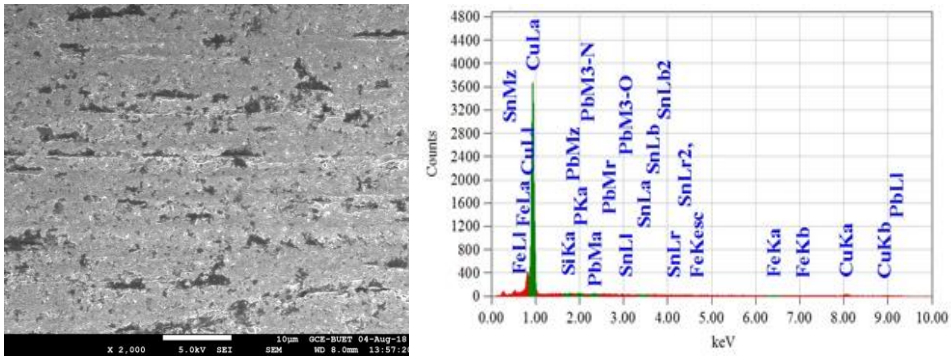

(c)

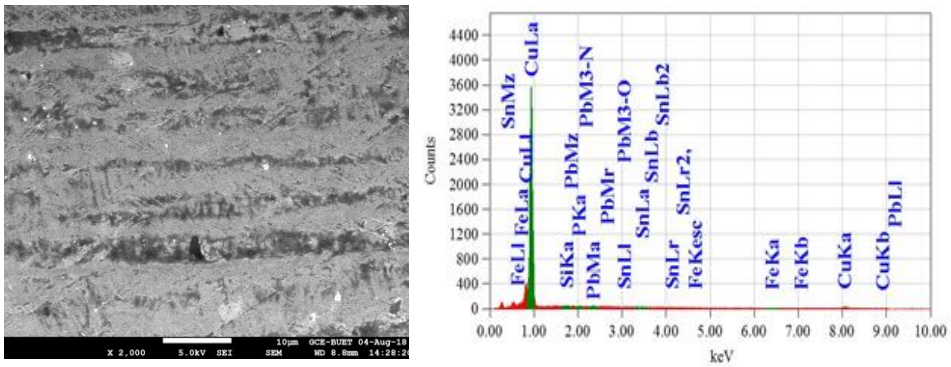

(d)

Fig. 11. SEM images along with EDX spectra of cold rolled (a) pure Cu, (b) binary Cu-Sn alloy, (c) binary Cu-Pb alloy and (d) ternary Cu-Sn-Pb alloy

The corresponding EDX for each alloy conforms to the chemical composition listed in Table 1. The EDX of the matching SEM of Cu reveals the following chemical composition by weight percentage: 99.70% Cu, 0.09% Si and 0.21% P. The EDX scan reveals the following chemical composition by the weight percentage of Cu-Sn Alloy: 97.18% Cu, 1.14% Sn, 0.25 % Pb and 0.41% Si and 0.82% Fe. Similarly, the Cu-Pb alloy shows 97.52% Cu, 1.00% Pb, 0.20% Si, 0.22% P, and 1.07% Fe. The solder affected Al-Sn-Pb alloy consists of 96.99% Cu, 0. 75% Sn, 0.95% Pb, 0.15% Si, 0.29% P, and 0.87% Fe.

4. Conclusions

The main findings from the present study of fractional recrystallization behaviour of pure copper containing the elements of Sn-PB solder alloy are as follows:

- The presence of the elements of Sn-Pb solder alloy shows positive effect on the fractional recrystallization characteristic of commercially pure copper. The cold-rolled pure copper (75% deformation) is found to recrystallize 99.4% when it is annealed for a period of one hour at 700°K, whereas the same for the ternary copper alloy (Cu-Sn-Pb) is found to take place only 89.5% under the same condition. More specifically, when the results are analyzed in the perspective of individual constituent elements of the solder alloy, the effect of tin is identified to be more influential than lead in preventing the recrystallization of copper. This is because of

the fact that FCC Cu and BCC Sn lattice alloys exhibit different supersaturated solid solution patterns of higher internal stress than those of both similar lattices of Cu and Pb. Additionally, tin forms different intermetallic with Cu as well as trace impurities, but lead does not form any intermetallic with Cu.

- Under isothermal annealing, the resistivity of heavily cold-rolled alloys demonstrates an initial drop in resistivity, followed by a small increase, and finally a slow but steady decrease. The initial drop of this property is associated with dislocation, rearrangement, and recovery phenomena; secondly, the minor increase is related to different intermetallic formation; and finally, a slow and steady decrease in resistivity is due to particle coarsening, grain coarsening, and recrystallization. The rate of change of resistivity for the ternary Cu alloy is all concomitances the highest because both the elements Sn and Pb play a part in creating dislocation density.
- Pure Cu demonstrates almost identical fractional recrystallization behavior in micro-hardness data and JMAK analyses. The Sn added alloy shows the greater divergence between the two methods, followed by the individual Pb addition. In the early stage of annealing, various trace impurities create diverse intermetallic, particularly with Sn. Furthermore, Sn has a different crystal structure than Cu as well as Pb. As a result, the binary Cu-Pb alloy is less stable than the Cu-Sn alloy as well as the ternary copper alloy. When both the elements of the solder alloy are present in Cu, the resulting alloy eventually makes the discrepancy between the two methods quite significant.
- All the alloys reached a state of almost fully recrystallized after annealing at 700°K for a period of 1800 seconds, but the ternary copper alloy demonstrates a higher fraction of the dissolved second phase in the microstructure and developed grain boundaries.

Acknowledgement

The corresponding author would like to express sincere gratitude to the authority of the International University of Business Agriculture and Technology, Dhaka, for their encouragement in promoting research activities in the university. Their efforts in fostering collaboration with other institutions are also worthy of recognition.

References

[1] Islak S, Çalıgülü U, Hraam HRH, Özorak C, Koç V. Electrical conductivity, microstructure and wear properties of Cu-Mo coatings. Research on Engineering Structures and Materials, 2019; 5(2): 137-146. http://dx.doi.org/10.17515/resm2018.58is0716

[2] Kaiser S, Kaiser MS. Influence of Aluminium and Zinc Additives on the Physical and Thermal Behaviour of Cast Copper. Journal of Sustainable Structures and Materials, 2020; 3(1): 1-9. http://dx.doi.org/10.26392/SSM.2020.03.01.001

[3] Afifeh M, Hosseinipour SJ, Jamaati R. Manufacturing of pure copper with extraordinary strength-ductility-conductivity balance by cryorolling and annealing. CIRP Journal of Manufacturing Science and Technology, 2022; 37: 623-632. https://doi.org/10.1016/j.cirpj.2022.03.010

[4] Davis JR. Introduction and Overview of Copper and Copper Alloys. Metals Handbook Desk Edition (2nd Edition), ASM International, Materials Park, Ohio, USA, 1998. https://doi.org/10.31399/asm.hb.mhde2.9781627081993

[5] Liu J, Liu J, Wang X. Study on Phase Transformation Dynamics, Microstructure, and Properties of the Cu-2.7Ti-2.5-Ni-0.8V Alloy. Archives of Metallurgy and Materials, 2023; 68(4): 1383-1390. https://doi.org/10.24425/amm.2023.146204

[6] Kaiser S, Kaiser MS. Impact of cold plastic deformation and thermal post-treatment on the physical properties of copper based alloys Al-bronze and α-brass. Journal of Acta Metallurgica Slovaca, 2021; 12(2): 103-108. https://doi.org/10.36547/ams.27.3.951

[7] Zeng C, ZhangB, Ettefagh AH, Wen H, Yao H, Meng WJ, Guo S. Mechanical, thermal, and corrosion properties of Cu-10Sn alloy prepared by laser-powder-bed-fusion additive manufacturing. Additive Manufacturing, 2020; 35: 1-8. https://doi.org/10.1016/j.addma.2020.101411

[8] Khan AA, Kaiser S, Kaiser MS. Electrochemical corrosion performance of copper and uniformly alloyed bronze and brass in 0.1 M NaCl solution. Revista Mexicana de Física, 2023; 69(5):1-10. 10.31349/RevMexFis.69.051002

[9] Constantinescu S, Popa A, Groza JR, Bock I. New high-temperature copper alloys. Journal of Materials Engineering and Performance, 1996; 5: 695-698. https://doi.org/10.1007/BF02646904

[10] Haque MS, Khan SAR, Kaiser MS. Effect of Sc and Zr on Precipitation Behaviour of Wrought Al- Bronze. IOP Conference Series Materials Science and Engineering, 2022; 1248(1):1-12. https://doi.org/10.1088/1757-899X/1248/1/012037

[11] Tylecote RF. The Prehistory of Metallurgy in the British Isles: 5, 1st edition, 1986, Taylor & Francis, London, UK. https://doi.org/10.4324/9781351199476

[12] Rahman MM, Ahmed SR, Kaiser MS. On the investigation of reuse potential of SnPb-solder affected copper subjected to work-hardening and thermal ageing. Materials Characterization, 2021; 172(3): 1-19. https://doi.org/10.1016/j.matchar.2021.110878

[13] Ahmed A, Iqbal N, Kaiser MS, Ahmed SR. Thermo-mechanical and optical characteristics of cold-rolled copper with natural melting impurities. AIP Conference Proceedings, 2021; 2324(1): 0300171-7. https://doi.org/10.1063/5.0037516

[14] Kaiser MS. Fractional recrystallization behavior of impurity-doped commercially pure aluminum. Journal of Energy, Mechanical, Material, and Manufacturing Engineering, 2020; 5(2): 37-46. https://doi.org/10.22219/jemmme.v5i2.11675

[15] Minggao Y, Qingsui W, Kuangdi X. Recovery and Recrystallization. In: Xu, K. (eds) The ECPH Encyclopedia of Mining and Metallurgy. 2023, Springer, Singapore. https://doi.org/10.1007/978-981-19-0740-1_931-1

[16] Benchabane G, Boumerzoug Z, Gloriant T, Thibon I. Microstructural characterization and recrystallization kinetics of cold rolled copper. Physica B: Condensed Matter, 2011; 406(10): 1973-1976, https://doi.org/10.1016/j.physb.2011.02.068

[17] Rokon N, Haque MS, Kaiser MS. On the mechanical behaviour of thermally affected non-heat-treatable aluminium alloys, Journal of Chemical Technology and Metallurgy, 2023; 58(6): 1153-1162. https://doi.org/10.59957/jctm.v58i6.156

[18] Shen K, Guo M, Wang M. Recrystallization characteristics of a fine grained copper alloy. Materials Chemistry and Physics, 2010; 120(2-3): 709-714. https://doi.org/10.1016/j.matchemphys.2009.12.019

[19] Haessner F. Hoschek G, Tölg G. Stored energy and recrystallization temperature of rolled copper and silver single crystals with defined solute contents. Acta Metallurgica, 1979; 27(9): 1539-1548. https://doi.org/10.1016/0001-6160(79)90176-7

[20] Kaiser MS. Precipitation and softening behaviour of cast, cold rolled and hot rolling prior to cold rolled Al-6Mg alloy annealed at high temperature. Journal of Mechanical Engineering, The Institution of Engineers, Bangladesh, 2015; ME45(1): 32-36. https://doi.org/10.3329/jme.v45i1.24381

[21] Freudenberger J, Kauffmann A, Klaub H, Marr T, Nenkov K, Sarma VS, Schultz L. Studies on recrystallization of single-phase copper alloys by resistance measurements. Acta Materialia, 2010; 58(7): 2324-2329. https://doi.org/10.1016/j.actamat.2009.12.018

[22] Tarasiuk J, Gerber P, Bacroix B. Estimation of recrystallized volume fraction from EBSD data. Acta Materialia, 2002; 50(6): 1467-1477. https://doi.org/10.1016/S1359-6454(02)00005-8

[23] Benchabane G, Boumerzoug Z, Thibon I, Gloriant T. Recrystallization of pure copper investigated by calorimetry and microhardness. Materials Characterization, 2008; 59(10): 1425-1428, https://doi.org/10.1016/j.matchar.2008.01.002

[24] Rokon SMN, Kaiser MS, Shorowordi KM. Fractional recrystallization kinetics in non-heat-treatable aluminium alloys. AIP Conference Proceedings, 2021; 2324(1): 0600061-6. https://doi.org/10.1063/5.0037948

[25] Kalu PN, Waryoba DR. A JMAK-microhardness model for quantifying the kinetics of restoration mechanisms in inhomogeneous microstructure. Materials Science and Engineering: A, 2007; 464(1-2): 68-75, https://doi.org/10.1016/j.msea.2007.01.124

[26] Morozova A, Dolzhenko A, Odnobokova M, Zhilyaev AP, Belyakov A, Kaibyshev R. Annealing Behavior and Kinetics of Primary Recrystallization of Copper. Defect and Diffusion Forum, 2018; 385, 343-348. https://doi.org/10.4028/www.scientific.net/ddf.385.343

[27] Zhang Z, Wang R, Peng C, Feng Y, Wang X, Wu X, Cal Z. Effect of elevated-temperature annealing on microstructureand properties of Cu−0.15Zr alloy, Transactions of Nonferrous Metals Society of China. 2021; 31(12): 3772-3784. https://doi.org/10.1016/S1003-6326(21)65763-1

[28] Alaneme KK, Okotete EA. Recrystallization mechanisms and microstructure development in emerging metallic materials: A review. Journal of Science: Advanced Materials and Devices, 2019; 4(1): 19-33. https://doi.org/10.1016/j.jsamd.2018.12.007

[29] Yang P, He D, Shao W, Tan Z, Guo X, Lu S, Anton K. Study of the microstructure and mechanical properties of Cu–Sn alloys formed by selective laser melting with different Sn contents. Journal of Materials Research and Technology, 2023; 24: 5476-5485. https://doi.org/10.1016/j.jmrt.2023.04.198

[30] Kim JC, Ko BH, Moon IH. On some physical properties of nanostructured Cu-Pb alloy prepared by mechanical alloying. Nanostructured Materials, V1996; 7(8): 887-903, https://doi.org/10.1016/S0965-9773(96)00059-1

[31] Leineweber A. The Cu–Sn System: A Comprehensive Review of the Crystal Structures of its Stable and Metastable Phases. journal of Phase Equilibria and Diffusion, 2023; 44, 343-393. https://doi.org/10.1007/s11669-023-01041-3

[32] Humphreys FJ, Hatherly M. Recrystallization and related annealing phenomena. 2nd edition, 2004, Elsevier, Oxford, UK. https://doi.org/10.1016/B978-0-08-044164-1.X5000-2

[33] Kaiser MS. Fractional Recrystallization Behaviour of Al-Mg Alloy with Different Sc Addition Content. International Journal of Materials Science and Engineering, 2014; 2(2): 136-140, 2014. https://doi.org/10.12720/ijmse.2.2.136-140

[34] Dutta S, Kaiser MS. Recrystallization Kinetics in Aluminum Piston. Procedia Engineering, 2014; 90: 188-192. https://doi.org/10.1016/j.proeng.2014.11.835

[35] Jiang Y, Gu RC, Peterlechner M, Liu YW, Wang JT, Gerhard Wilde, Impurity effect on recrystallization and grain growth in severe plastically deformed copper. Materials Science and Engineering: A, 2021; 824: 141786-790, https://doi.org/10.1016/j.msea.2021.141786

[36] Gierlotka W, Chen S, Lin S. Thermodynamic description of the Cu–Sn system. Journal of Materials Research, 2007; 22(11): 3158-3165. https://doi.org/10.1557/JMR.2007.0396

[37] Li R, Wang E, Zuo X. Co-Precipitation, Strength and Electrical Resistivity of Cu–26 wt % Ag–0.1 wt % Fe Alloy. Materials, 2017, 10(12): 1-17. https://doi.org/10.3390/ma10121383

[38] Peng J, Li J, Liu B, Fang Q, Liaw PK. Origin of thermal deformation induced crystallization and microstructure formation in additive manufactured FCC, BCC, HCP metals and its alloys. International Journal of Plasticity, 2024; 172: 1-21. https://doi.org/10.1016/j.ijplas.2023.103831